

## Supplementary Materials for

### **A new dynamical systems perspective on atmospheric predictability: Eastern Mediterranean weather regimes as a case study**

Assaf Hochman\*, Pinhas Alpert, Tzvi Harpaz, Hadas Saaroni, Gabriele Messori

\*Corresponding author. Email: [assafhochman@yahoo.com](mailto:assafhochman@yahoo.com)

Published 5 June 2019, *Sci. Adv.* **5**, eaau0936 (2019)

DOI: 10.1126/sciadv.aau0936

#### **This PDF file includes:**

Table S1. Snow events in Jerusalem from the available TIGGE database (27, 28).

Table S2. The eight CMIP5 models used in the present study with the following information: Modeling center (or group), institute ID, model name, and horizontal resolution (°) following Taylor *et al.* (29).

Table S3. Model rank scores for each synoptic group with respect to the NCEP/NCAR reanalysis.

Table S4. CMIP5 models and NCEP/NCAR reanalysis transition probabilities for the different synoptic groups.

Table S5. Model mean absolute differences for the transition probabilities of each synoptic group with respect to the NCEP/NCAR reanalysis (%).

Fig. S1. The study region following Alpert *et al.* (7).

Fig. S2. Meteogram from ECMWF's EPS (Ensemble Prediction System) forecast system initialized on Wednesday, 11 December 2013, 00:00 UTC at the location of Jerusalem (31.9°N 35.2°E; 815 m).

Fig. S3. Mean SLP composite maps from NCEP/NCAR reanalysis as classified by the Alpert *et al.* (7) synoptic classification algorithm for 1986–2005.

**Table S1. Snow events in Jerusalem from the available TIGGE database (27, 28).**

The predicted and observed data is for the entire event. The ECMWF forecast was initialized on the first day of the event.

<b>Snow Event (DD/MM/YY)</b>	<b>12/12/10</b>	<b>2/3/12</b>	<b>12/12/13</b>	<b>7/1/15</b>	<b>21/2/15</b>
<i>d – local dimension</i>	12.21	12.07	13.71	5.88	10.71
<i>Θ - inverse persistence</i>	0.57	0.78	0.71	0.71	0.82
<b>ECMWF predicted IMS observed precipitation</b>	~15mm 46mm	~45mm 185mm	~50mm 227mm	~22mm 54mm	~50mm 105mm
<b>ECMWF predicted IMS observed Snow depth</b>	0cm 20cm	0cm 10cm	~10cm 50cm	~5cm 5cm	~10cm 25cm
<b>Forecast initialized at:</b>	11/12/10 00UTC	28/2/12 00UTC	11/12/13 00UTC	7/1/15 00UTC	18/2/15 00UTC

**Table S2. The eight CMIP5 models used in the present study with the following information: Modeling center (or group), institute ID, model name, and horizontal resolution (°) following Taylor *et al.* (29).**

<b>Modeling Center (or Group)</b>	<b>Institute ID</b>	<b>Model Name (short name)</b>	<b>Resolution (°)</b>
Canadian Centre for Climate Modelling and Analysis, Canada	CCCMA	CanESM2 (CANESM)	2.79 X 2.81
National Centre for Atmospheric Research, USA	NCAR	CCSM4 (CCSM)	0.94X 1.25
Met Office Hadley Centre, England	MOHC	HadGEM2-CC (HadGEM2CC) HadGEM2-ES (HadGEM2ES)	1.25 X 1.88 1.25 X 1.88
Institut Pierre-Simon Laplace, France	IPSL	IPSL-CM5A-LR (IPSL)	1.9 X 3.75
Max Planck Institute for Meteorology, Germany	MPI-M	MPI-ESM-LR (MPI)	1.87 X 1.88
Meteorological Research Institute, Japan	MRI	MRI-CGCM3 (MRI)	1.12X 1.13
Norwegian Climate Centre, Norway	NCC	NORES1-M (NORES1)	1.9 X 2.5

**Table S3. Model rank scores for each synoptic group with respect to the NCEP/NCAR reanalysis.** The scores are calculated such that:  $R(d) = D(d) / \max[D(d)]$  and  $R(\theta) = D(\theta) / \max[D(\theta)]$ , where D represents the difference between the median values of d or  $\theta$  of each model and the NCEP/NCAR values for each synoptic group. Max refers to the value for model with the largest difference D. The lower the score, the closer the model is to the reanalysis<sup>30</sup>.

One can then compute a global score as:  $R(\text{global}) = (R(d) + R(\theta)) / 2$ , presented in the table. The averages and standard deviations (STD) of all the global scores for each model are also shown.

Synoptic groups are Red Sea Troughs (RSTs), Persian Troughs (PTs), Highs (H), Cyprus Lows (CLs) and Sharav Lows (SLs).

<b>Model/Score</b>	<b>RST</b>	<b>PT</b>	<b>H</b>	<b>CL</b>	<b>SL</b>	<b>Average (STD)</b>
<b>MPI</b>	0.22	0.42	0.15	0.23	0.49	<b>0.30 (0.14)</b>
<b>CANESM</b>	0.32	0.31	0.36	0.27	0.30	<b>0.31 (0.03)</b>
<b>MRI</b>	0.59	0.67	0.11	0.06	0.41	<b>0.37 (0.25)</b>
<b>CCSM</b>	0.42	0.42	0.36	0.27	0.83	<b>0.46 (0.19)</b>
<b>HadGEM2CC</b>	0.26	0.65	0.56	0.88	0.57	<b>0.58 (0.20)</b>
<b>HadGEM2ES</b>	0.17	0.72	0.62	0.92	0.54	<b>0.59 (0.25)</b>
<b>IPSL</b>	0.93	0.85	0.91	0.81	0.63	<b>0.82 (0.11)</b>
<b>NORES</b>	0.78	0.89	0.78	0.80	1.00	<b>0.85 (0.09)</b>

**Table S4. CMIP5 models and NCEP/NCAR reanalysis transition probabilities for the different synoptic groups.** Synoptic groups are as in table S3. The table provides the same information as Fig. 6 but in numerical format.

<b>CANESM</b>	<b>RST</b>	<b>PT</b>	<b>H</b>	<b>CL</b>	<b>SL</b>
<b>RST</b>	47.14	0.58	26.29	23.75	2.24
<b>PT</b>	0.97	72.15	21.51	5.27	0.11
<b>H</b>	18.69	7.27	52.73	18.52	2.79
<b>CL</b>	10.32	2.86	23.67	62.19	0.95
<b>SL</b>	12.14	3.57	12.86	59.29	12.14

<b>CCSM</b>	<b>RST</b>	<b>PT</b>	<b>H</b>	<b>CL</b>	<b>SL</b>
<b>RST</b>	48.95	2.24	25.16	22.13	1.51
<b>PT</b>	2.90	73.43	20.00	3.57	0.10
<b>H</b>	17.73	7.96	56.62	15.87	1.82
<b>CL</b>	9.37	1.64	25.35	63.32	0.32
<b>SL</b>	14.29	2.04	12.24	47.96	23.47

<b>HadGEM2CC</b>	<b>RST</b>	<b>PT</b>	<b>H</b>	<b>CL</b>	<b>SL</b>
<b>RST</b>	54.65	0.00	16.36	26.67	2.31
<b>PT</b>	0.27	56.30	24.66	18.77	0.00
<b>H</b>	17.29	4.09	52.49	23.37	2.76
<b>CL</b>	13.33	2.80	14.87	67.90	1.10
<b>SL</b>	19.05	0.00	12.93	52.38	15.65

<b>HadGEM2ES</b>	<b>RST</b>	<b>PT</b>	<b>H</b>	<b>CL</b>	<b>SL</b>
<b>RST</b>	53.32	0.23	20.62	24.11	1.72
<b>PT</b>	0.23	60.41	21.95	17.42	0.00
<b>H</b>	21.40	4.67	48.38	22.77	2.79
<b>CL</b>	13.18	2.84	13.88	69.20	0.89
<b>SL</b>	21.67	0.00	12.50	55.00	10.83

<b>IPSL</b>	<b>RST</b>	<b>PT</b>	<b>H</b>	<b>CL</b>	<b>SL</b>
<b>RST</b>	64.29	3.55	13.60	17.76	0.81
<b>PT</b>	11.07	72.32	4.50	11.94	0.17
<b>H</b>	27.29	2.33	49.17	19.13	2.08
<b>CL</b>	16.23	1.41	8.25	73.49	0.61
<b>SL</b>	16.90	2.82	2.82	67.61	9.86

<b>MPI</b>	<b>RST</b>	<b>PT</b>	<b>H</b>	<b>CL</b>	<b>SL</b>
<b>RST</b>	51.35	0.98	21.25	23.71	2.70
<b>PT</b>	3.15	52.45	34.97	8.92	0.52
<b>H</b>	18.47	8.07	52.31	19.32	1.83
<b>CL</b>	11.82	2.54	21.33	63.00	1.31
<b>SL</b>	21.92	0.00	15.75	47.26	15.07

<b>MRI</b>	<b>RST</b>	<b>PT</b>	<b>H</b>	<b>CL</b>	<b>SL</b>
<b>RST</b>	50.84	0.11	27.15	20.35	1.56
<b>PT</b>	3.57	32.14	39.29	25.00	0.00
<b>H</b>	20.96	0.34	59.65	17.73	1.31
<b>CL</b>	11.34	0.29	20.66	67.15	0.55
<b>SL</b>	15.15	0.00	14.14	49.49	21.21

<b>NORES</b>	<b>RST</b>	<b>PT</b>	<b>H</b>	<b>CL</b>	<b>SL</b>
<b>RST</b>	56.58	1.81	22.52	17.42	1.68
<b>PT</b>	3.76	72.59	19.06	4.47	0.12
<b>H</b>	15.63	6.78	60.13	15.59	1.87
<b>CL</b>	9.82	1.36	22.56	65.85	0.41
<b>SL</b>	18.80	0.75	11.28	32.33	36.84

<b>NCEP/NCAR</b>	<b>RST</b>	<b>PT</b>	<b>H</b>	<b>CL</b>	<b>SL</b>
<b>RST</b>	55.14	5.25	26.76	11.73	1.12
<b>PT</b>	3.43	70.42	22.16	3.66	0.32
<b>H</b>	25.48	19.98	40.87	12.26	1.41
<b>CL</b>	15.19	8.55	30.58	44.92	0.76
<b>SL</b>	11.59	31.88	24.64	27.54	4.35

**Table S5. Model mean absolute differences for the transition probabilities of each synoptic group with respect to the NCEP/NCAR reanalysis (%).** The averages and standard deviations (STD) of all synoptic groups for each model are also shown. The “Weighted Average” column shows an average score where the biases for individual transitions are weighted by the frequency of the transition itself. Synoptic groups are as in table S3.

<b>Model/Synoptic group</b>	<b>RST (%)</b>	<b>PT (%)</b>	<b>H (%)</b>	<b>CL (%)</b>	<b>SL (%)</b>	<b>Average (STD) (%)</b>	<b>Weighted Average (%)</b>
<b>CANESM</b>	5.26	1.33	7.80	6.99	16.04	7.48 (4.82)	7.89
<b>CCSM</b>	4.32	1.20	7.91	7.36	16.89	7.54 (5.26)	8.24
<b>NORESM</b>	3.08	1.32	9.22	8.37	17.80	7.96 (5.77)	8.71
<b>MPI</b>	5.43	7.30	7.57	7.45	16.31	8.81 (3.83)	8.75
<b>HadGEM2ES</b>	5.19	5.50	7.76	9.77	17.61	9.17 (4.54)	10.6
<b>HadGEM2CC</b>	6.45	7.04	9.63	9.33	17.44	9.98 (3.93)	10.2
<b>IPSL</b>	6.07	7.12	7.06	11.85	20.36	10.49 (5.33)	12.5
<b>MRI</b>	3.78	15.44	9.70	8.89	16.95	10.95 (4.76)	11.0

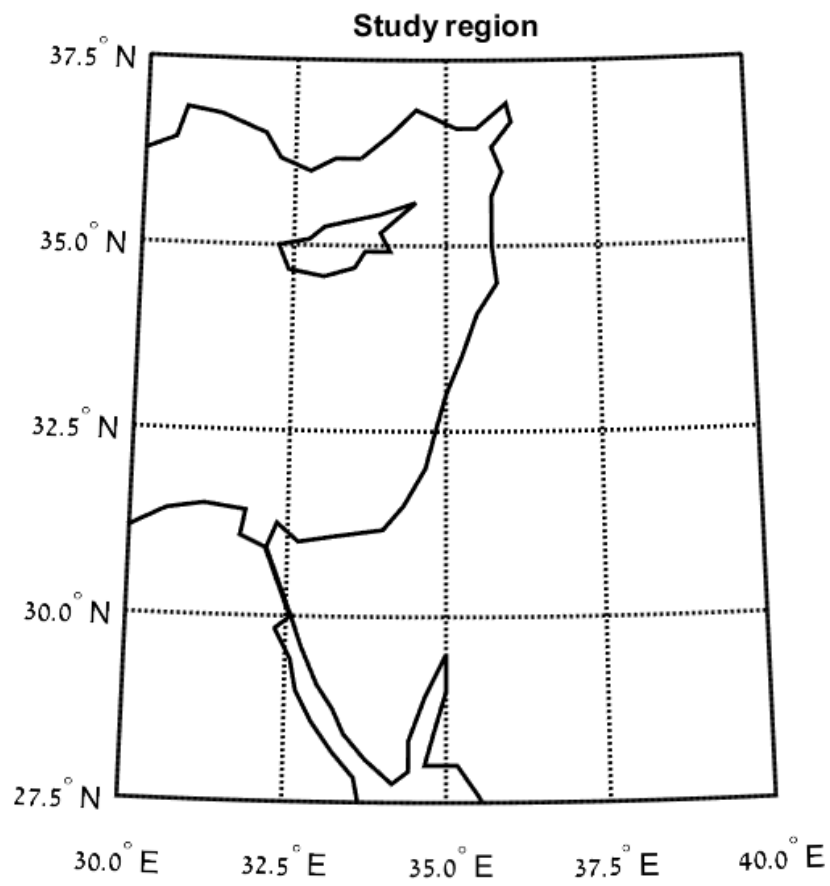


**Fig. S1.** The study region following Alpert *et al.* (7).



EPS Meteogram  
 Jerusalem 31.9°N 35.2°E (EPS land point) 815 m  
 Deterministic Forecast and EPS Distribution Wednesday 11 December 2013 00 UTC

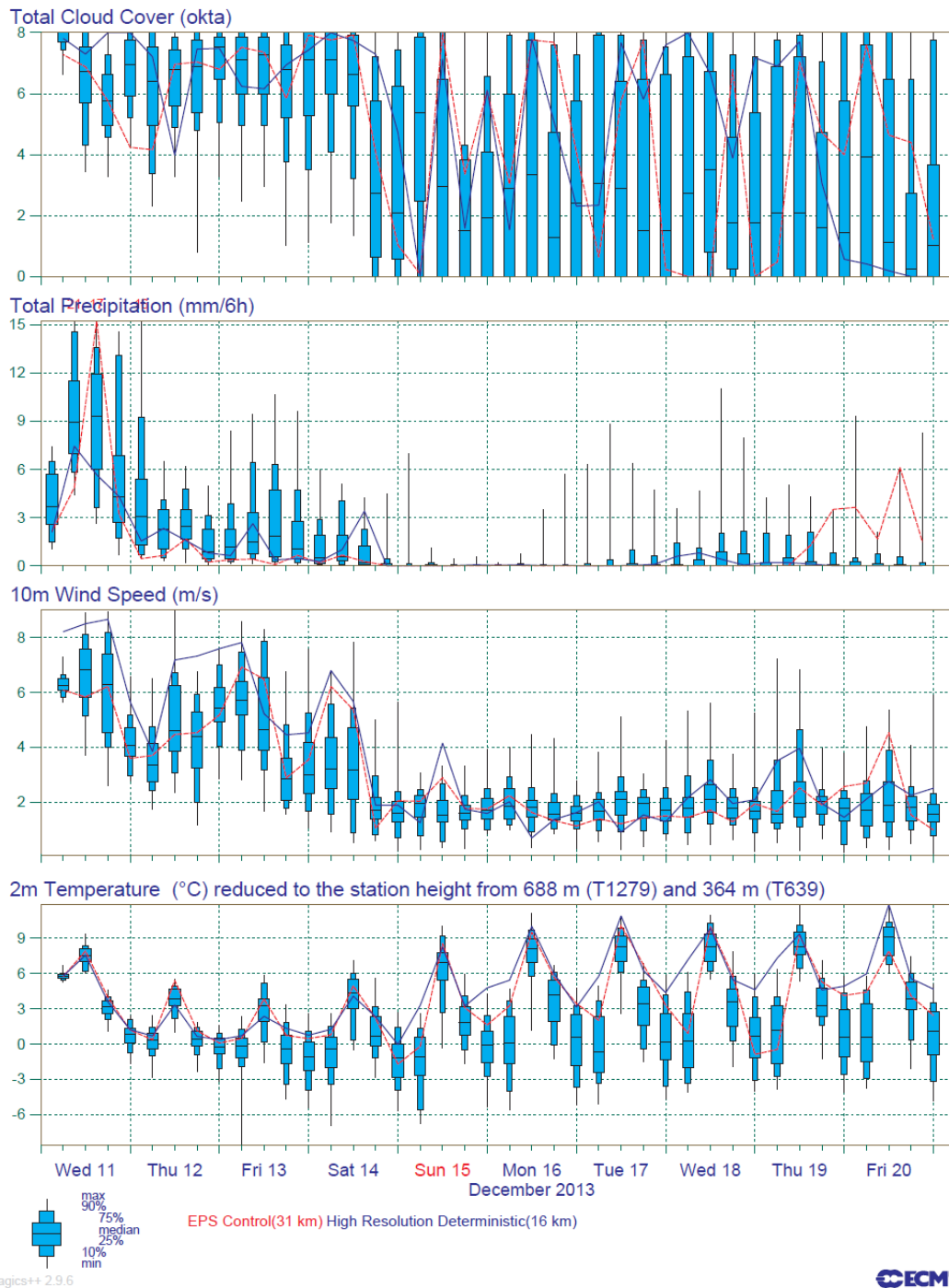


**Fig. S2. Meteogram from ECMWF's EPS (Ensemble Prediction System) forecast system initialized on Wednesday, 11 December 2013, 00:00 UTC at the location of Jerusalem (31.9°N 35.2°E; 815 m).**

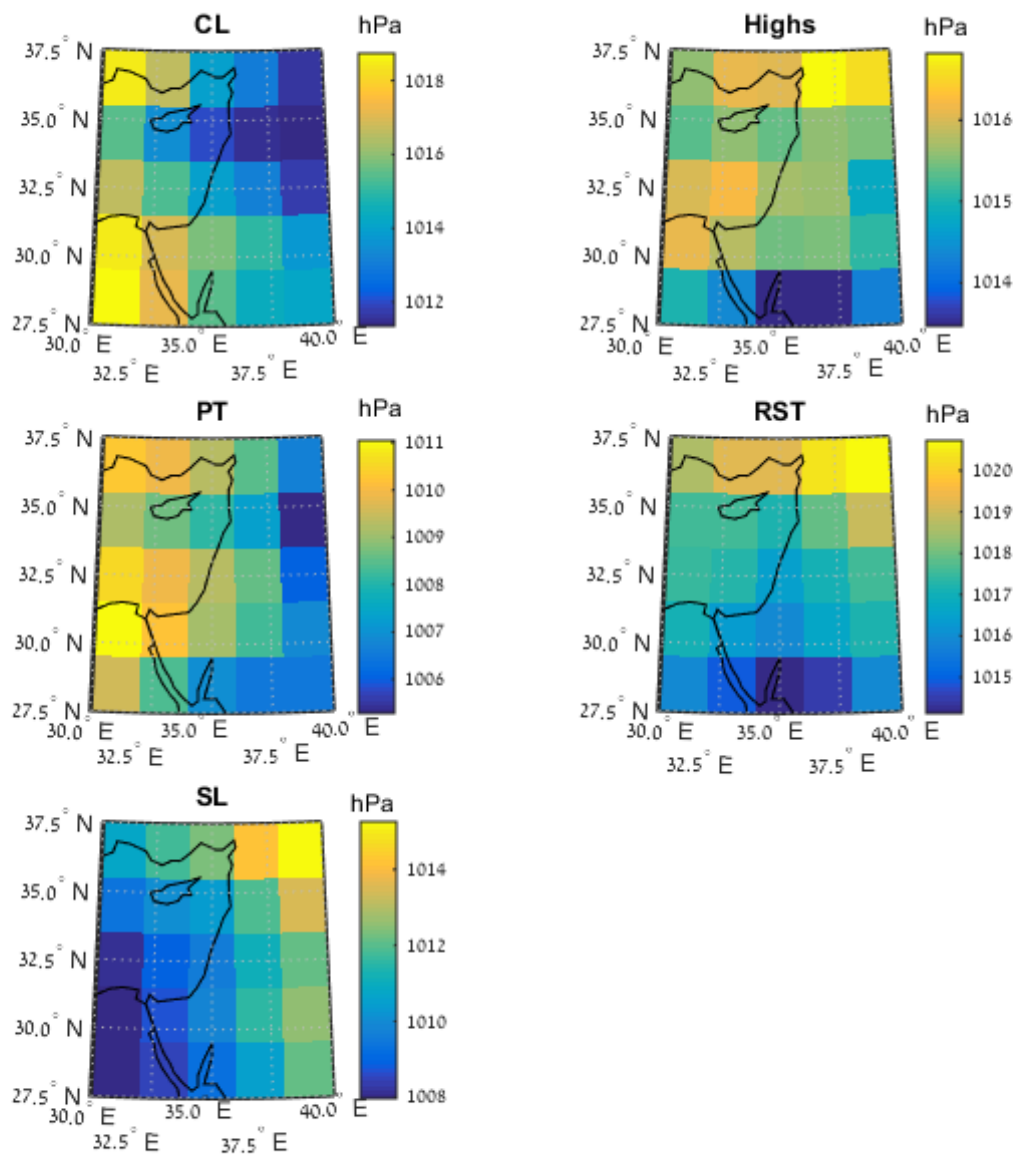


**Fig. S3. Mean SLP composite maps from NCEP/NCAR reanalysis as classified by the Alpert *et al.* (7) synoptic classification algorithm for 1986–2005. The synoptic systems are as in table S3.**